

Atlas guided segmentation of brain images via optimizing neural networks

Gene Gindi[†], Anand Rangarajan^{‡§} and I. George Zubal[‡]

[†]Department of Radiology
SUNY at Stony Brook
Stony Brook, NY 11794

[‡]Department of Diagnostic Radiology
Yale University School of Medicine
New Haven, CT 06510-3333

[§]Department of Computer Science
Yale University
New Haven, CT 06520-2158

Abstract

Automated segmentation of magnetic resonance (MR) brain imagery into anatomical regions is a complex task that appears to need contextual guidance in order to overcome problems associated with noise, missing data, and the overlap of features associated with different anatomical regions. In this work, the contextual information is provided in the form of an anatomical brain atlas. The atlas provides defaults that supplement the low-level MR image data and guide its segmentation. The matching of atlas to image data is represented by a set of deformable contours that seek compromise fits between expected model information and image data. The dynamics that deform the contours solves both a correspondence problem (which element of the deformable contour corresponds to which elements of the atlas and image data?) and a fitting problem (what is the optimal contour that corresponds to a compromise of atlas and image data while maintaining smoothness?) Some initial results on simple 2D contours are shown.

1 Introduction

There has been considerable interest in recent years in the possibility of segmenting anatomical structures as seen in three-dimensional (3D) high-resolution magnetic resonance (MR) scans. By “segment”, we imply the labelling of the image at every voxel with the correct anatomical descriptor(s). For example, a given voxel may be labelled with the symbol “caudate”, along with the label “striatum”, a structure that includes the caudate as its part. It may be argued that such a labelling is ill-defined in that a crisp anatomical boundary may not exist at the level of resolution of the MR image. Indeed, it may be argued that such boundaries may be hard to define even at a histological level. Nevertheless, it is obvious that such boundaries are often well defined (e.g. boundary of the ventricles) or, at worst, exist approximately, and in this initial work we simply ignore such difficulties.

There are many possible applications for a successful segmentation. In surgical planning, the identification and display of specific anatomical structures enables a surgeon to target or avoid such a structure in a surgical approach. A similar situation obtains in radiation therapy, where high-intensity beams of radiation must pass through the least damaging path of normal tissue in order to deposit dose in the target lesion.

Other applications are possibly more attractive. In many areas of psychiatric research [1], current hypotheses regarding forms of mental illness are posed in terms of morphometric measurements of brain structures; for example,

the volume of the ventricles in schizophrenics vs. non-schizophrenics. In such projects, the intended structure must currently be segmented by laborious and expensive human labor. If the patient database is large and the measurements subtle as in differential measurements, then an automated or even semi-automated method could be attractive in its repeatability, possible accuracy, and time savings. Automated segmentation may also find a use as a teaching tool. Software packages currently exist for the browsing of complex anatomical structures that have been previously hand-segmented. However, the automated segmentation of a new dataset for addition to the teaching tool could be quite useful.

In this paper, we present a new method for labelling anatomy that relies on an anatomical atlas to guide the segmentation. The representation of the problem and the resulting computations are inspired by our own research in neural-networks for model-based recognition [2], [3]. In Section 2, we give a brief mention of current anatomical segmentation techniques, and qualitatively describe our own approach. In Section 3, a mathematical model is presented and some initial results on a small 2D dataset are presented in Section 4. Finally, a brief discussion is found in Section 5.

2 Conventional and atlas-based segmentation techniques

In this section, we first give a brief description of other techniques that have been used in anatomical segmentation and then describe the motivation for our atlas-based scheme. Our model is presented in Section 4. (References to previous work are only representative – this is not intended as a complete survey.) We arbitrarily categorize previous methods by the terms: voxel-based, snakes, and geometric warping.

In voxel-based methods, the idea is to label individual voxels. A variety of techniques have been applied. Standard supervised pattern recognition techniques have been used in which the image value at each voxel, (possibly a vector of three values for an MR scan) is used as an input feature. Discriminant boundaries between anatomical types are derived using a training set obtained from supervised examples on the same image, or from other images. Other standard statistical techniques, both supervised and unsupervised, have been used [4], [5]. In related efforts, Markov Random Field (MRF) models [6] have been applied to the labelling problem. The MRF models are able to capture the notion that nearby labels are likely to be identical but change at organ boundaries. MRF techniques are voxel classification techniques though they incorporate the labels of nearby voxels to help determine the correct label of the voxel at hand.

“Snakes” are deformable contours that move across the image under mathematical forces that seek to corral anatomical regions. Typically, the mathematical representation of a snake is that of a closed contour; the pixels inside the contour are then considered to be members of a given region. Snakes are driven by dynamics that seek to minimize an objective function. The objective function contains terms that seek consistency of the snake with image features along with a degree of smoothness of the contour. A typical data-consistency term seeks to position the snake over a locus of high magnitude of intensity gradient in the image. The tacit presumption is that anatomical regions are conveniently determined by grey scale edges. By its very representation as a closed contour and by its smoothness, snakes overcome problems in edge-finding schemes for region delineation by avoiding the necessity to link edge fragments and by interpolating over noisy regions. Some examples of snakes include [7], [8]. Snakes may be modified to include specific information regarding the expected shape of the object sought by a given snake. For example Yuille [9] segments components of a face image (i.e. nose, ears, mouth etc.) with snakes whose objective functions are modulated to reflect the expected shapes. Other amendments for incorporating contextual information are possible.

Both of the above techniques operate directly on the image. A different approach makes use of the contextual information provided by an anatomical atlas to segment a test image. An atlas may be thought of as a correctly labelled exemplar of brain anatomy. The atlas itself is derived by hand labelling (by an expert) physical slices of brain tissue derived from a cadaver, or likewise by hand labelling a sequence of high resolution MR slices of a given patient. The patient then serves as an exemplar [10].

Warping techniques seek to label a test image by geometrically deforming a labelled atlas until it overlays the image. If a given brain image differed from the atlas by a simple rigid transformation, then a successful registration of atlas and image could accomplish the labelling; one need only apply to each image voxel the label of the associated atlas voxel. However, the atlas and image will differ by some general topology preserving geometric warping rather than a rigid registration. A more difficult goal is to search for the warping deformation that is smooth (not too tortuous) and is also consistent with image data. A key component of this approach is the definition of consistency. One may seek image features, such as easily delineated points, contours or surfaces, and warp the atlas so that this subset is well matched. The assumption is that the deformation will “carry along” the matching of all other features of interest since the underlying optimal deformation is presumably smooth. Warping approaches have been applied to medical data by [11] and [12].

Our proposed technique shares features with both the snakes and warping approaches. In our method, the atlas is comprised of sets of 2D labelled *atlas contours*. The image is pre-processed to derive a set of approximate *image contours* that represent strong edges in the MR data. Segmentation is formulated as an optimization problem in which a third *deformable contour* is fitted based on a compromise fit to both the atlas and image contours. The image contour is held fixed and is thus a constant in this particular formulation. The atlas contour is also held fixed after an initial rigid registration with the image contour. Recent work on anatomical segmentation that shares some of the above features can be found in [13].

The problem has the flavor of matching curves. In our approach, the curves (contours) are *not* represented parametrically. Instead, they are represented as a list of coordinates. Our match metric involves summing up contributions from *corresponding* pairs of points on the two curves. Since the correspondence is not known *a priori*, we have to solve for correspondence between points in addition to evaluating the match metric; i.e. we have a simultaneous correspondence–regression problem.

More specifically, in our model, the correspondence between the atlas and deformable contour is presumed known. However, the correspondence between the deformable contour and the image contour is not presumed to be known in advance. The optimization seeks a deformable contour that satisfies three criteria: (i) the deformable contour matches the atlas contour, (ii) the deformable contour is itself smooth, and (iii) the points on the deformable contour correspond to points on the image contour such that the two contours are well matched. The variables of the optimization are thus the coordinates of the deformable contour as well as a *correspondence matrix* that associates points on the deformable contour with corresponding points on the image contour. In a sense, the deformable contour acts as an intermediary in establishing correspondence between the *atlas* contour and the image contour.

The problem of simultaneous correspondence–regression arises frequently in neural nets where it is termed “deformable templates” [14]. Deformable templates have been applied to problems in character recognition [15], labelling bubble chamber tracks, and problems in computer vision. Neural nets have been successfully used in problems such as these that involve a combination of a discrete optimization problem (correspondence) and a continuous optimization problem (regression).

Table 1: Table of symbols used

$\{\mathbf{x}_i\}$	set of points specifying the image contour
$\{\mathbf{y}_a\}$	set of points specifying the deformable contour
$\{\mathbf{z}_a\}$	set of points specifying the atlas contour
$\{M_{ai}\}$	correspondence matrix
δ	smoothing parameter
γ	data fit parameter
β	control parameter

3 A neural net method

In this work, we attack a reduced version of the problem. The atlas contour of a single structure (striatum) in a selected transverse slice is obtained from an atlas [16]. The image contour of the same structure (striatum) is obtained from a transverse MR slice of a given patient. Figure 1 shows the MR slice and the striatum. Rather than consider all possible transformations, we have taken an atlas contour that is roughly registered to the image contour.

The atlas, image and deformable contours are represented as lists of coordinates. In our representation, we have taken the number of atlas and deformable contour points to be the same. (This considerably simplifies the specification of the energy function.) As shown in Table 1, the image, deformable, and atlas contour points are specified by \mathbf{x}_i , \mathbf{y}_a , and \mathbf{z}_a respectively. The atlas and deformable contour points share the same index a since they are always in correspondence.

We now present the energy function for fitting a deformable contour to both atlas and image contours while establishing correspondence.

$$E(\{\mathbf{y}_a\}, \{M_{ai}\}) = \frac{1}{2} \sum_a \|\mathbf{z}_a - \mathbf{y}_a\|^2 + \frac{\delta}{2} \sum_a \|\mathbf{y}_{a+1} - \mathbf{y}_a\|^2 + \frac{\gamma}{2} \sum_{ai} M_{ai} \|\mathbf{x}_i - \mathbf{y}_a\|^2 \quad (1)$$

where

$$\sum_a M_{ai} = 1, \quad \sum_i M_{ai} \leq 1 \text{ and } M_{ai} \in \{0, 1\}, \quad \forall a, i. \quad (2)$$

In (1), the first term expresses the fact that the deformable contour point \mathbf{y}_a should be close to the atlas contour point \mathbf{z}_a . The second term is a smoothness constraint on \mathbf{y}_a . The third term expresses the fact that \mathbf{y}_{ai} should be close to its corresponding image point \mathbf{x}_i . The actual correspondence is represented by a binary matrix M_{ai} which equals unity when point \mathbf{x}_i corresponds to the point \mathbf{y}_a . In our model, we take the number of atlas points to be greater than the number of image data points (factor of two). Then, M_{ai} expresses the fact that for every data point there is at least one corresponding deformable contour point but not vice-versa. This accounts for the constraints in (2).

It would seem that a binary correspondence matrix M_{ai} would be very brittle for this kind of problem since only one deformable contour point is ultimately associated with each image point. Since the number of deformable contour points \mathbf{y}_a outnumber the image points, we could instead associate more than one \mathbf{y}_a to each \mathbf{x}_a . The deformable points associated with the image point would all fall within a neighborhood of the image point.

It has been shown [17] that an effective energy function implicitly containing the effect of M_{ai} can be directly derived from statistical physics. The startling feature of this approach is that a correspondence matrix M_{ai} can be

constructed for each setting of a control parameter, β . This constructed matrix has the feature of allowing multiple associations between the deformable contour points and the image points and the strength of these associations depend on the value of the parameter. The effective energy function is

$$F(\{\mathbf{y}_a\}) = \frac{1}{2} \sum_a \|\mathbf{z}_a - \mathbf{y}_a\|^2 + \frac{\delta}{2} \sum_a \|\mathbf{y}_{a+1} - \mathbf{y}_a\|^2 - \frac{1}{\beta} \sum_i \log \sum_a \exp\left(-\frac{\beta\gamma}{2} \|\mathbf{x}_i - \mathbf{y}_a\|^2\right) \quad (3)$$

The only difference between (1) and (3) is in the third term. M_{ai} has been eliminated and instead we have the $\log \sum \exp(\cdot)$ expression. An immediate connection between (1) and (3) can be established by “running steepest descent” on our new energy function. This obtains:

$$\frac{d\mathbf{y}_a}{dt} = -(\mathbf{y}_a - \mathbf{z}_a) + \delta(\mathbf{y}_{a+1} - 2\mathbf{y}_a + \mathbf{y}_{a-1}) - \gamma \sum_i M_{ai}(\mathbf{y}_a - \mathbf{x}_i) \quad (4)$$

where we have identified

$$M_{ai} = \frac{\exp\left(-\frac{\beta\gamma}{2} \|\mathbf{x}_i - \mathbf{y}_a\|^2\right)}{\sum_b \exp\left(-\frac{\beta\gamma}{2} \|\mathbf{x}_i - \mathbf{y}_b\|^2\right)}. \quad (5)$$

This expression for M_{ai} exhibits the feature of multiple associations each of whose strength depend on the value of the global parameter β .

We now have all the elements in place to specify our algorithm. Once the atlas and image contours are approximately registered, we insert them into the energy function that is then minimized with respect to the deformable contour \mathbf{y}_a . The energy function is first minimized for low values of β and then β is increased. Any standard descent algorithm can be used to minimize the energy function (we used conjugate gradient) at a fixed value of β .

4 Results

Preliminary registration of the atlas contour to the image contour was achieved via a log-polar mapping. The translation between the centers of gravity of the two contours was first obtained. Then the coordinates were transformed into log-polar space and scale and rotation were crudely obtained. Finally, a small *ad-hoc* visually guided rotation and translation was performed. For our small problem, this kind of registration replaces the more ambitious multi-modality registration schemes found in the medical imaging literature [18].

During the execution of the algorithm, the parameter γ was not kept constant. Instead, we increased it gradually according to

$$\gamma(\beta) = \gamma_0 \left(1 - \frac{\beta_{\min}}{\beta}\right) \quad (6)$$

where β_{\min} is the first setting of β . This allows the constraint to be imposed gradually. The parameter β itself was varied according to the following schedule.

$$\beta_{\text{new}} = (1 - \alpha)\beta_{\text{max}} + \alpha\beta_{\text{old}} \quad (7)$$

In all experiments, $\beta_{\min} = 1.0/8192.0$, $\beta_{\text{max}} = 100.0$ and $\alpha = 0.01$.

Figures 2(a) and (b) show the original atlas and image contours, respectively. The number of atlas points was 29 and the number of image data points was 15. It is clearly seen that the scale and translation of the two figures are not the same (as seen in the axes of display). However, the orientation of the two contours seems similar.

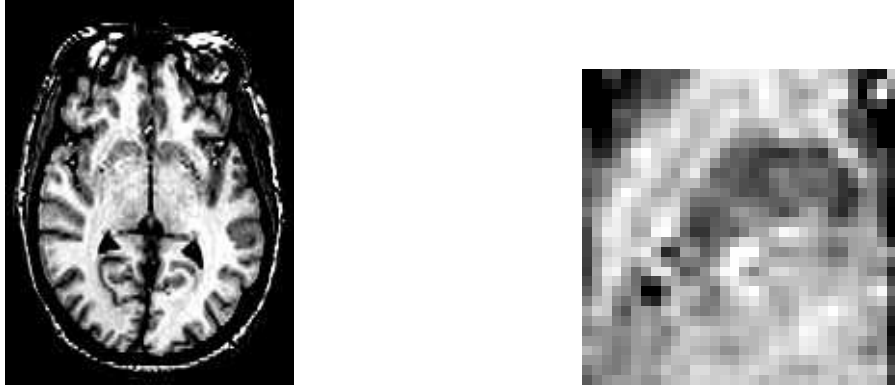


Figure 1: Left: Transverse MR slice, Right: Striatum

In Figure 3(a), an approximately registered version of the two contours in Figure 2 is shown. Then in Figure 3(b), the results of running our network for the parameter settings of $\delta = 1$ and $\gamma_0 = 1$ are shown. This is the choice for which no energy term in (1) is favored. In the figure, the deformable contour is displayed as a thick line. The deformable contour is relatively smooth and does not show excessive adherence to the atlas or image data.

In Figure 4(a), the image energy term is favored by setting $\gamma_0 = 10$ with the same levels of smoothness and adherence to the atlas. Naturally, the deformable contour adheres more closely to the image and is markedly not smooth. Now, in Figure 4(b), the smoothness is increased to half the strength of the image term ($\delta = 5$) and we see that new deformable contour is smoother than that in Figure 4(a). When we continue to increase the smoothing term ($\delta = 10$), keeping the image term constant ($\gamma_0 = 10$), an interesting thing happens: the new deformable contour is very smooth and for the most part stays within *both* the atlas and image contours. This seems reasonable since the smoothing action is as dominant as the image term.

Finally, as shown in Figure 5(b), when we flip to the other extreme – no smoothing – with $\delta = 0$ and $\gamma_0 = 1$, we get a jagged contour that tries to adhere to both the atlas and the image. For this choice of parameter, it mostly adheres to the atlas, but local fidelity to the image can also be seen. The case when $\gamma_0 = 0$ (no image contour) is not very interesting and is not shown here.

5 Discussion

The segmentation of brain images into anatomical regions poses a complex task with potentially useful payoffs. While the problem is far from trivial, the fact that brain anatomy is topologically ordered and grossly similar in shape details from patient to patient makes the problem perhaps tractable. It appears that a variety of approaches may be needed to successfully segment the brain; for example, the grey – white matter boundaries may be difficult to model with an atlas as there is no “prototypical” boundary of this sort.

References

- [1] N. Andreasen, “Brain Imaging: Applications in Psychiatry”, *Science*, vol. 239, pp. 1381–1388, March 1988.

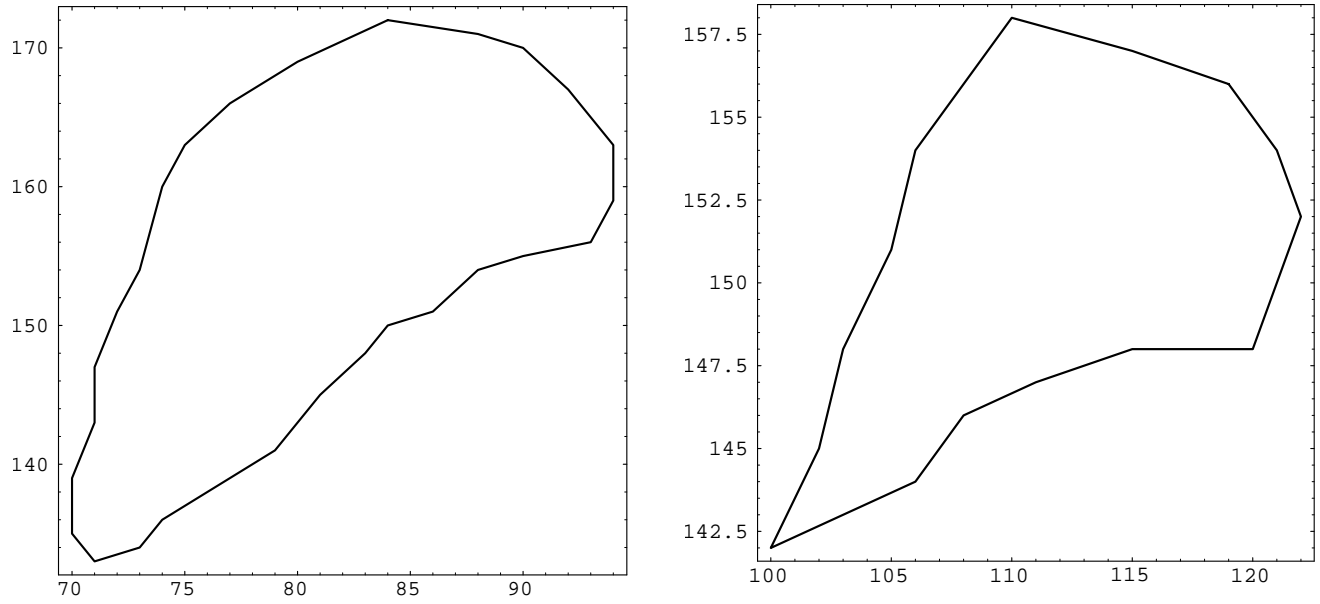


Figure 2: Left: Atlas contour (original), Right: Image contour (original)

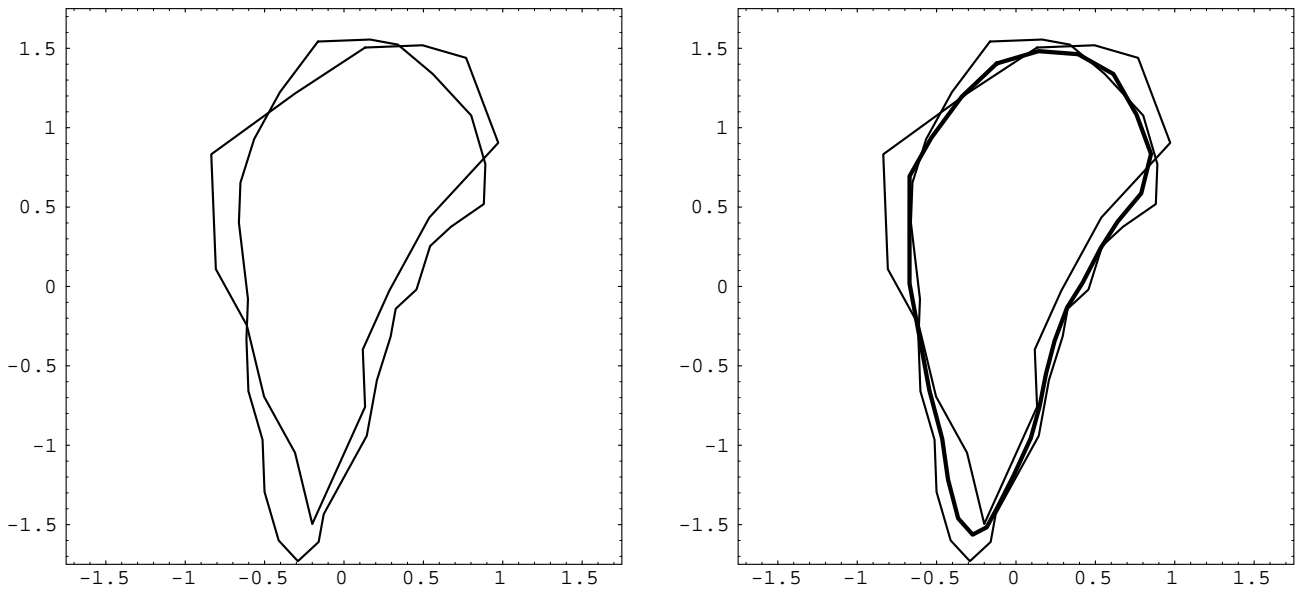


Figure 3: Left: Partially registered contours, Right: Deformable contour with $\delta = 1$ and $\gamma_0 = 1$

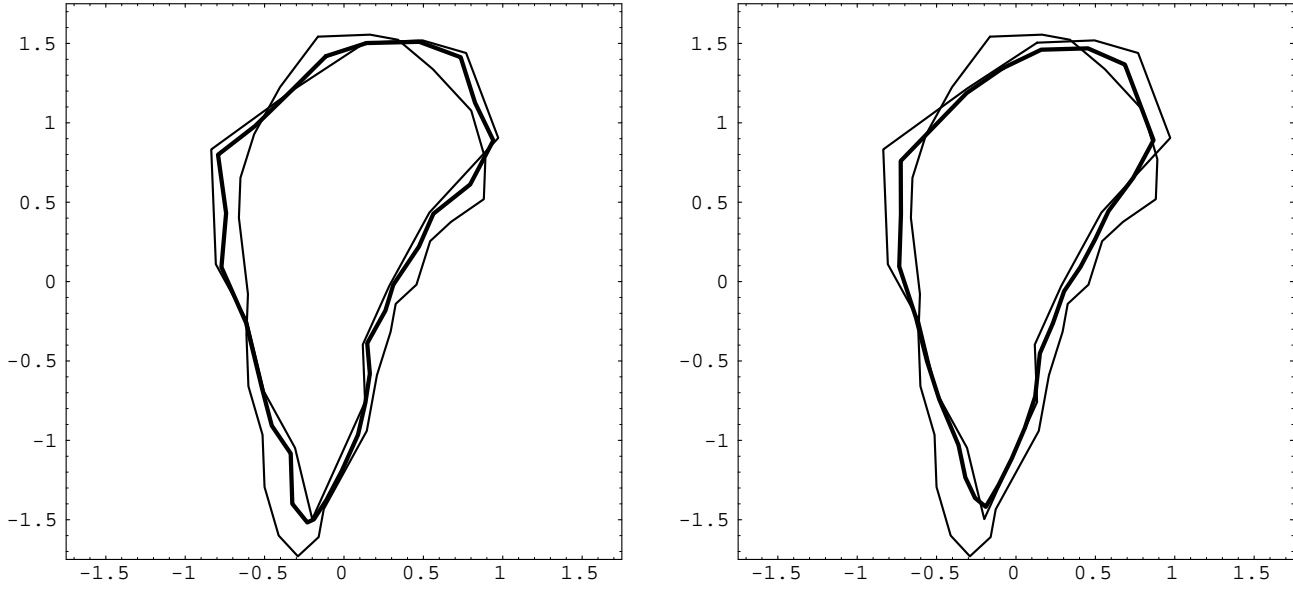


Figure 4: Left: Deformable contour with $\delta = 1$ and $\gamma_0 = 10$, Right: Deformable contour with $\delta = 5$ and $\gamma_0 = 10$

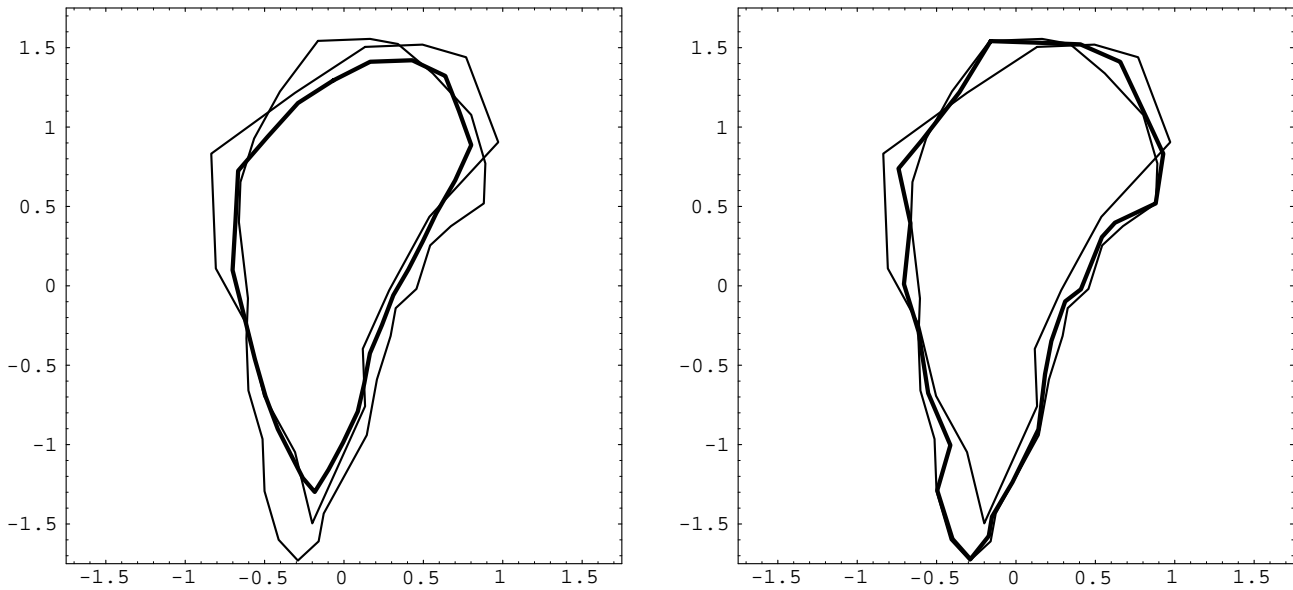


Figure 5: Left: Deformable contour with $\delta = 10$ and $\gamma_0 = 10$, Right: Deformable contour with $\delta = 0$ and $\gamma_0 = 1$

- [2] E. Mjolsness, G. Gindi, and P. Anandan, "Optimization in Model Matching and Perceptual Organization", *Neural Computation*, 1, pp. 218–229, 1989.
- [3] G. Gindi, E. Mjolsness, and P. Anandan, "Neural Networks for model-based recognition", In P. Antognetti and V. Milutinovic, editors, *Neural Networks: Concepts, Applications and Implementations, vol III*, pp. 144–173, Prentice-Hall, 1991.
- [4] G. Gerig, J. Martin, R. Kikinis, O. Kubler, M. Shenton, and F. Jolesz, "Automating Segmentation of Dual-Echo MR Head Data", In A. C. F. Colchester and D. J. Hawkes, editors, *Information Processing in Medical Imaging*, pp. 175–185, Springer-Verlag, 1991.
- [5] H. Cline, W. Lorenen, R. Kikinis, and F. Jolesz, "Three-Dimensional Segmentation of MR Images of the Head Using Probability and Connectivity", *Journal of Computer Assisted Tomography*, 14(6), pp. 1037–1045, Nov/Dec 1990.
- [6] R. Leahy, T. Hebert, and R. Lee, "Applications of Markov Random Fields in Medical Imaging", In D. Ortendahl and J. Llacer, editors, *Information Processing in Medical Imaging*, pp. 1–14, Wiley-Liss, 1991.
- [7] L. Staib and J. Duncan, "Boundary Finding with Parametrically Deformable Models", *IEEE Trans PAMI*, vol. 14(11), pp. 1061–1075, November 1992.
- [8] D. Terzopoulos, J. Platt, A. Barr, and K. Fleischer, "Elastically Deformable Models", *Computer Graphics*, vol. 21(4), pp. 205–214, July 1987.
- [9] A. Yuille, D. Cohen, and P. Hallinan, "Feature Extraction from Faces Using Deformable Templates", *International Journal of Computer Vision*, 8(2), pp. 99–111, 1992.
- [10] I. G. Zubal, G. Gindi, M. Lee, C. Harrell, and E. Smith, "High Resolution Anthropomorphic Phantom for Monte Carlo Analysis of Internal Radiation Sources", In *Proceedings of the Third Annual IEEE Symposium on Computer-Based Medical Systems*, pp. 540–547, 1990.
- [11] R. Bajcsy and S. Kovacic, "Multiresolution Elastic Matching", *Computer Vision, Graphics and Image Processing*, vol. 46, pp. 1–21, 1989.
- [12] M. Moshfeghi, "Elastic matching of Multimodality Medical Images", *Computer Vision, Graphics and Image Processing*, vol. 53(3), pp. 271–282, May 1991.
- [13] S. Sandor and R. Leahy, "Recognition of brain images from magnetic resonance images", In *Proceedings 26th Asilomar Conference on Signals, Systems and Computers*, Pacific Grove, CA, October 1992.
- [14] A. Yuille, "Generalized Deformable Models, Statistical Physics, and Matching Problems", *Neural Computation*, 2, pp. 1–24, 1990.
- [15] G. Hinton, C. Williams, and M. Revow, "Adaptive Elastic Models for Hand-Printed Character Recognition", In J. Moody, S. Hanson, and R. Lippmann, editors, *Advances in Neural Information Processing Systems 4*, pp. 512–523, Morgan-Kaufman, 1992.
- [16] J. Talairach and P. Tournoux, "*Co-Planar Stereotaxic Atlas of the Human Brain*", Thieme Medical Publisher, Inc., New York, 1988.
- [17] P. D. Simic, "Statistical mechanics as the underlying theory of 'elastic' and 'neural' optimisations", *Network*, 1, pp. 89–103, 1990.
- [18] I. G. Zubal, H. Tagare, L. Zhang, and J. Duncan, "3-D Registration of Intermodality Medical Images", In J. H. Nagel and W. M. Smith, editors, *Proceedings of the Annual International Conference of the IEEE Engineering in Medicine and Biology Society*, pp. 293–294, 1991, vol. 13.